CA- 6 | 55

MILITARY TECHNICAL COLLEGE

CAIRO - EGYPT

NUMERICAL COMPUTATIONS OF TURBULENT AND SWIRLING FLOWS IN AXI-SYMMETRICAL COMBUSTOR

Tharwat M. FARAG

ABSTRACT

Numerical, marching procedure is presented for the calculations of the transport processes in two-dimensional flow characterized by the presence of one coordinate in which physical influences are exerted in only one direction. The differential equations for the transport of mass and momentum with the help of the Prandtle mixing length for turbulence have been solved using the discretization technique. The boundary of the reverse flow zone, which was measured, was introduced to the calculations as an inner boundary.

The calculations has been performed for the forward flow passing in the annular space confined by the combustor wall and the reverse flow zone boundary. The boundary of the reverse flow zone was detected accurately, simply and easily by a special flow direction detector probe designed by the author. To verify the calculations, the results were compared with the measured axial and tangential velocities that measured by the Laser Doppler Anemometer.

The axial and tangential velocities distributions and the dimensionless stream lines were estimated. The predicted results indicated good agreement with the experimental results.

1. INTRODUCTION

The swirling flows are commonly used in industrial furnaces and gas turbine combustors to increase flame stability and combustion intensity. In the case of strong swirl, the adverse axial pressure gradient is sufficiently large to result in reverse flow along the axis and setting up of an internal recirculation zone /1-5/. Then, the flow inside the combustor can be considered two-directional flows; the first one , the backward flow is found in the combustor core and the second, the forward flow is found near the combustor wall. The later is the main flow direction.

Turbulent swirling flows are now widely found in many engineering applications. The swirling flows properties can be obtained either by numerical

* Lecturer, Mechanical Power Department , Faculty of Engineering and Technology-Port Said, Suez Canal University, EGYPT.

computation or by direct measurements which in fact are difficult. There are number of accurate numerical procedures, the most successful one is the finite difference technique. However, if numerical computations are applied, it has needed to compare their predictions with experimental results.

The most published researches concerning the numerical methods were oftenly compared with the experimental results. Only the boundary and initial conditions were used as an input data for computations /6-10/. Here in this work, the measured boundary of the reverse flow zone formed in swirling flow was added to the other input data and was taken as an inner annular boundary. Therefore, the flow under consideration was confined by the combustor wall at the outer edge and confined by the inner boundary (where the axial velocity component is equal zero). The calculations were proceeded only for the forward flow. Using the measured inner boundary in this work leaded the calculations to be reliable. And also the computation time was relatively too short compared with the others /6-10/. Here, the calculation time for predicting the axial and tangential velocities distributions was about 8.4 sec.

For verification, the predicted results were compared with the experimental one made by the author and they can be found in reference/5/. The reverse flow zone boundary was measured directly and simply by the flow direction detector probe designed by the author and more details can be found also in reference/5/.

2. CALCULATION PROCEDURES

2.1. THE DIFFERENTIAL EQUATIONS

The differential equations that used in this calculation express the implications of the relevant conservation laws for steady axi-symmetrical flows. Although the flow is turbulent, a time-average values of the variables are taken. The mixing, brought about by the fluctuating components, will be expressed in term of effective shear stress.

The flow region of interest, as an our assumption , will be considered to lie between two surfaces, for which the subscripts I(internal) and E(external) will be used. the internal surface is the surface of the boundary of reverse flow zone as deduced experimentally. The external surface is the wall surface, which its entrance takes the shape of cone and follows by cylindrical surface to the outlet.

The streamwise co-ordinate Z will be approximately parallel to the streamlines. The non-dimensional stream function ω is defined as;

$$\omega = (\Psi - \Psi_I) / (\Psi_E - \Psi_I) \qquad (1)$$

Where $\psi(r) = \int Urdr$ for fixed Z is employed as the independent variable across the layer. The conservation equations of axial and tangential momentums and stagnation enthalpy in the Z - ω coordinate system posses the common form as published in reference/11/;

$$\frac{\partial \phi}{\partial Z} + (a + b\omega) \frac{\partial \phi}{\partial \omega} = \frac{\partial}{\partial \omega} (c \frac{\partial \phi}{\partial \omega}) + d \qquad (2)$$

Where the quantity ϕ stands for any of the typical dependent variables; axial and tangential velocities and stagnation enthalpy.

The computation was performed and was based on the Genmix-4 version of Patankar-Spalding Parabolic Computer Programme/11/. The necessary modifications were introduced to render the computations suitable for the prediction of swirling flows through confined passage.

The coefficients a and b are functions of Z alone. The term c embodies the transport law appropriate to the entity ϕ and is a function of Z, ω and the variable ϕ. d is the term on the right-hand side which does not contain $\partial\phi/\partial\omega$. The definitions of terms a, b, c and d can be found in Patankar and Spalding /11/.

We shall solve this equation by step-by-step forward integration. Therefore, at every step in the integration, the values of ϕ will be known at discrete values of ω and at one value of Z, the procedure will be to obtain the values of ϕ at the same values of ω , but at a downstream values of Z. By repeating of this basic operation, the whole field of interest can be covered. The discrete values of ω and Z, which are decided beforehand, define a grid; a portion of this is shown in Fig.1. Points U and D represent respectively the upstream and downstream points at a given ω ; points at nearby values of ω will be called U_+ , U_- , D_+ , D_- . The dashed lines 1 and 2 are the lines of constant ω . These two lines together with the two lines of constant Z, define the control volume(shown shaded).

Rather than solve the swirl equation in the Eq.2, the diffusion term of that equation was rewritten in terms of V_t/r instead of $V_t.r$ so as to eliminate the otherwise troublesome source term d of that equation. The swirl equation then becomes;

$$\frac{\partial}{\partial Z}(rV_t) + (a + b\omega) \frac{\partial}{\partial \omega}(rV_t) = \frac{\partial}{\partial \omega}(cr^2 \frac{\partial}{\partial \omega}(V_t/r)) \qquad (3)$$

The dependent variable of tangential momentum is $V_t.r$ and not V_t.

Swirling flows exhibit pressure variations normal to the axis of symmetry. The lateral pressure gradient is given by the equation;

$$\frac{\partial P}{\partial r} = \rho V_t^2 / r \qquad (4)$$

Therefore, the axial-pressure calculation has to be combined with that of the lateral pressure variation.

2.2. INITIAL AND BOUNDARY CONDITIONS

The flow enters the combustor from an annular space of inner and outer diameters 0.07 and 0.10 m respectively. The inlet axial velocity profile was assumed uniform. The inlet tangential velocity profile is commonly expressed in a forced vortex form as V_t = constant x r. This constant varies as a function of the swirl number. The inlet air flow rate is given by 0.075 Kg/s.

The axial and tangential velocities distributions at the combustor wall were equal zero. The tangential velocity at the combustor center line was also zero but the gradient of axial velocity is zero. At the boundary of the referse flow zone(R.F.Z.), the axial velocity is zero but the tangential velocity is not. The inlet temperature of the air was assumed constant and equal 300 K. The combustor wall was impermeable, adiabatic and its temperature was constant at 300 K. The equation of the stagnation enthalpy was solved only for examining the calculation procedure. The temperature inside the combustor at all the grid points was uniform and equal to 300 K because the velocity variations were not large.

2.3. THE FINITE DIFFERENCE EQUATIONS AND ITS SOLUTION

The set of parabolic equations prescribed by Eq.2 and 3 are then solved numerically by replacing them by finite difference equation. These equations are to be solved by a marching-integration procedure. Therefore, at every step in the integration, the values of $\emptyset$ will be known at discrete values of ω for one value of Z; then the values of $\emptyset$ at the same values of ω can be obtained but at a slightly greater value of Z (Z + dZ). By step-wise repeating of this basic operation, the whole field of interest can be covered. The discrete values of ω , which are decided beforehand, define a grid. The finite-difference equation is obtained by expressing each term in the parent partial differential equation as an integrated average over a small control volume defined by the grid. the integrals were evaluated by assuming that dependent variables posses a profile which is made up of chain with straight line links. The resultant finite difference equation takes the form :

$$\emptyset = A\,\emptyset_{++} + B\,\emptyset_{--} + C \qquad (5)$$

Where A, B and C are functions of ω differences, the values of $\emptyset$ at the upstream edge and the coefficients a, b, c and d. The equations are then solved for each forward step by use of a simple successive substitution technique (Tri-Diagonal Matrix Algorithm). The solution is marched downstream until the whole field of flow has been computed.

To prevent any negative coefficients, the high-lateral-flux modification /11/, was included. The dependent variables at the wall were linked to those at the nearest grid node from the wall by equations which are consistent with the logarithmic law of the wall.

3. COMPARISON OF PREDICTIONS WITH EXPERIMENTAL DATA

The construction of the combustion chamber is shown in Fig.2. It shows the boundary of the reverse flow zone. There are two flow directions; the forward and the backward flows. The backward flow is formed by the effect of the swirler and is found in the combustor core, but the forward flow is found near the inner surface of the combustor. More details about the combstor dimensions and the swirler construction can be found in reference /3/. The flow enters the combustor through a stabilizing cone of 30°. Figure 2 shows also the region wherein the calculations were performed. The calculations were proceeded for the forward flow only, which is confined at the inner surface by the measured boundary of the R.F.Z. and at the outer surface by the combustor wall. The boundary of the R.F.Z. is the boundary at which the axial velocity component is zero, or at which the forward flow reverses its direction.

The inlet air flow rate was 0.075 Kg/s, and the average mass flow rate of the recirculating air was assumed equal 0.1 to 0.2 of the inlet flow rate at swirl number of 0.50 /12/. Therefore, the calculations were proceeded for air flow rate increased by a ratio equals to 0.15.

Figure 3 shows the calculated mean-average axial velocity and pressure drop distributions with the axial distance for no swirl (S=0.0). The mean-average velocity , at given axial distance, equals the mean of the velocities at the radial distances.

The mean velocity decreases exponentially. Inside the divergent part of the combustor(stabilyzing cone), the mean velocity decreased strongly due to the change in the flow areas. It reaches 2.0 m/s at axial distance of about 0.14 m (at the cone end). The corresponding pressure was decreased . The pressure difference, Δp (difference between the pressure inside the combstor and the inlet pressure) increased up to axial distance where the cone ends. From the cone end to the combustor end, the pressure and the mean velocity were slightly decreased.

The mean axial and tangential velocities distributions with the radial distance at two different axial distances and swirl number 0.50 are shown in Fig.4 and Fig.5. The calculated results were compared with the measured one that were published by the author in reference /5/. The calculations can be found at the wright hand side of the edge of the R.F.Z. There is no calculation at the left hand side of the edge of the R.F.Z. The axial velocity enhanced from zero at the boundary of the R.F.Z. as shown in the upper part of Fig.4. The calculated axial velocity distribution is quite agreement with the measured values. In the lower part of this figure the tangential velocity has a value not zero at the R.F.Z. boundary. The tangential velocity increased with the radial distance and reached its maximum value near the combustor wall.

In figure 4 also, the radius of the R.F.Z. is large therefore, the region of calculation is small. At another axial distance where the radius of the R.F.Z. is relatively small and equals 0.047 m, the comparison of results are shown in Fig.5. The mean axial velocities are smaller than of Fig.4 and the reversed axial velocities are also smaller. The tangential velocities of Fig.4 and 5 are slightly different.

The calculated mean and axial velocities at different axial distances 0.15, 0.29 and 0.40 m for swirl number 0.50 are shown in Fig.6. These axial distances were chosen so that the radius of the R.F.Z. decreases with the increase of axial distance. As the axial distance increased, the mean axial velocity decreased but the mean tangential velocity slightly decreased. For without swirl (S=0.0), Fig.7 shows the calculated results at different axial distances 0.10, 0.30 and 0.60 m. In the case of no swirl, the inlet air flows through annular space likes the case of with swirl but with swirler blade angle equals zero/5/. Therefore, the velocity distribution has a maximum value at certain radius near the wall. at Z=0.10 m, the radius of the cone wall is 0.10 m as shown in the figure where the velocity equals zero. As the axial distance increased, the distribution of the velocity became uniform.

The calculated dimensionless stream lines for swirl numbers 0.0 and 0.50 are shown in Fig.8 and Fig.9, respectively. Without swirl, there is a small R.F.Z. found up to the axial distance 0.063 m as shown in Fig.8. This R.F.Z. was found due to the inner surface of the swirler according to its design. The inner surface acts as a bluff disc. The inlet flow rate was 0.075 Kg/s and the flow issued from an annular space to the convergent part. The dimensionless stream lines were drawn for ω =0.1, 0.3, 0.5, 0.7 and 0.9. Inside the combustor core the dimensionless stream lines were separated from each other because the velocities there were small but the velocities were relat ively high near the wall resulting in close stream lines.

For S=0.50, the R.F.Z. was found inside the whole length of the combustor from its inlet to the exit /5/.

The flow enters the combustor from annular space with axial and tangential momentums. The inlet flow rate was 0.075 Kg/s. The stream lines were close together due to the narrow passage for the flow, from the swirler exit up to axial distance 0.25 m. The lines were very close together in the cone passage and they separated gradually within the distance of 0.25 and 0.50 m. From Z=0.5 m to the combustor end, the size of R.F.Z. was increased due to the atmospheric effect (the combustor was opened to the atmosphere at its end), therefore the lines were again close together.

4. SUMMARY AND CONCLUSION

The coupling of the measured boundary of the reverse flow zone with the numerical computations based on the Genmix-4 version of Patankar-Spalding Parabolic Computer Programme, increases the validity of the computation with the measurements. The computations were carried on the forward flow region of the swirling flows, confined by the combustor wall at the outer edge and at the inner edge confined by the measured boundary of the reverse flow zone where the axial velocity was zero. The computations were performed for the flow with and without swirl. The calculated results indicated good agreement with the experimental results for the axial and tangential velocities distributions which were measured by the L.D.Anemometer.

5. REFERENCES

/1/ Beer,J.M. and Chigier,N.A., 'Combustion Aerodynamics' ,Applied Science Publishers, London, 1972.

/2/ Syred,N.and Beer,J.M.,'Combustion in Swirling Flows',A Review,Combust. and Flame 23, 143, 1974.

/3/ Farag,T.M., Arai,M.and Hiroyasu,H.,'Effect of Fuel Volatility on Spray Combustion',Proc. in 19th Symposium(Int.) on Combust.,p.511, 1982.

/4/ Rhode,D.L.,Lilley,D.G. and Mclaughlin,D.C.,'On the Prediction of Swirling Flowfields Found in Axisymmetric Combustor Geometries',ASME,104,378,1982.

/5/ Farag,T.M.,Arai,M.and Hiroyasu,H.,'Flow characterization With and Without Combustion in a Swirl Type Combustor',Int. Gas Turbin Congress,29,1982.

/6/ Khalil,E.E,Spalding,D.B and Whitelaw,J.H.,'The Calculation of Local Flow Properties in Two Dimensional Furnace',Int.J,Heat Mass Transfer,18,1975.

/7/ Patankar,S.V.and Spalding,D.B.,'A Computer Model for Three-Dimensional Flow in Furnaces',Proc. in 14th Int.Symposium On Combust., 1973.

/8/ Khalil,E.E.,'Numerical Computations of Turbulent Reacting Combustor Flow' Numerical Methods in Heat Transfer,John Wiley,Chapter 23, 1981.

/9/ Serag-Eldin,M.A. and Spalding,D.B.,'A Computational Procedure for Three Dimensional Recirculating Flows Inside Can Combustor',Numerical Methods in Heat Transfer,John Wiley, Chapter21, 1981.

/10/Kumar,D.S.,'Numerical Study of Swirling Flow Through Annular Diffusers Combust.in Eng., Inst. of Mech.Eng.,33, 1984.

/11/Patankar,S.V.and Spalding,D.B.,'Heat and Mass Transfer in Boundary layers' Intertext Books, London, 1970.

/12/Khalil,K.H.,F.M.EL-Mahallaway,andH.A.Moneib, 'Effect of Combustion Air Swirl on The Flow Pattern in a Cylindrical Oil Fired Furnaces',Proc.16th Symposium (Int.) on Combust.,135, 1976.

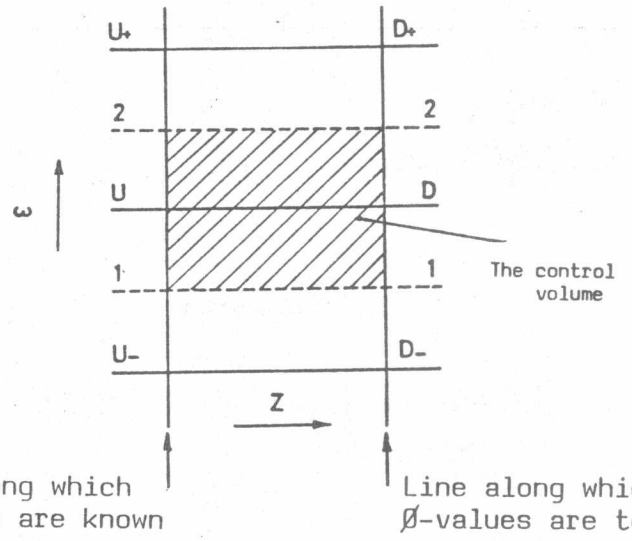

Fig.1 Location of points used in the difference equation and the control volume

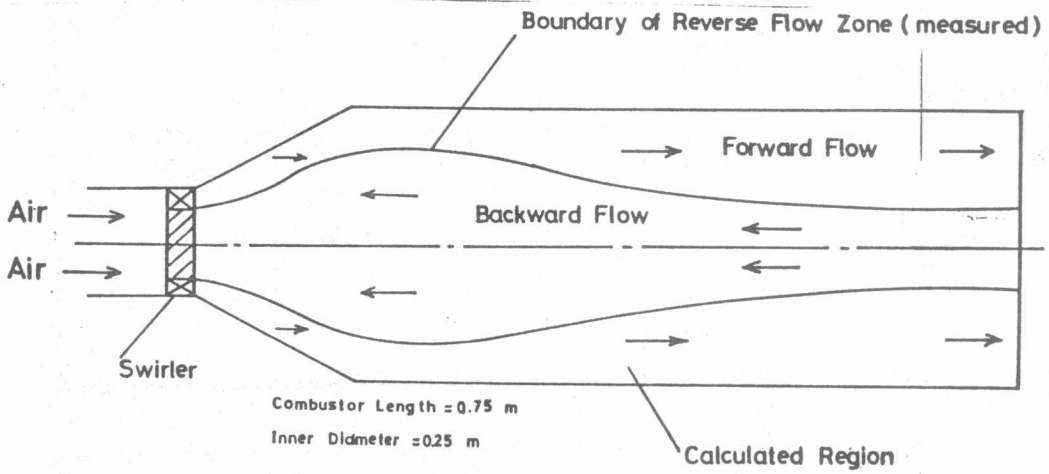

Fig.2 Combustion chamber construction shows backward and forward flow regions and the boundary of R.F.Z.

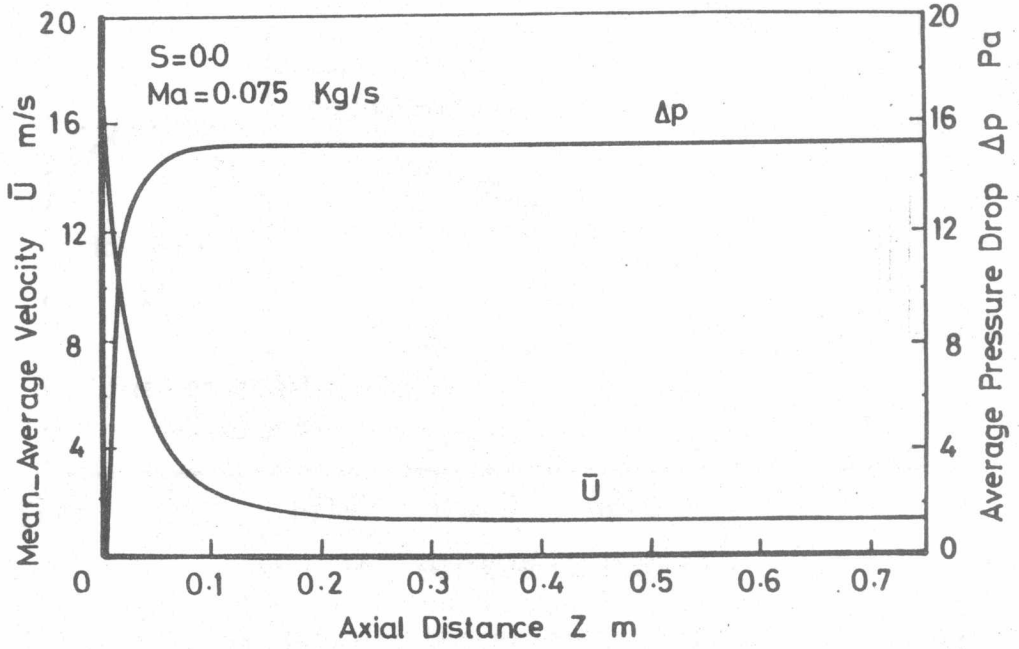

Fig.3 Mean-average axial velocity and average pressure drop with the axial distance, for S=0.0, Ma=0.075 Kg/s

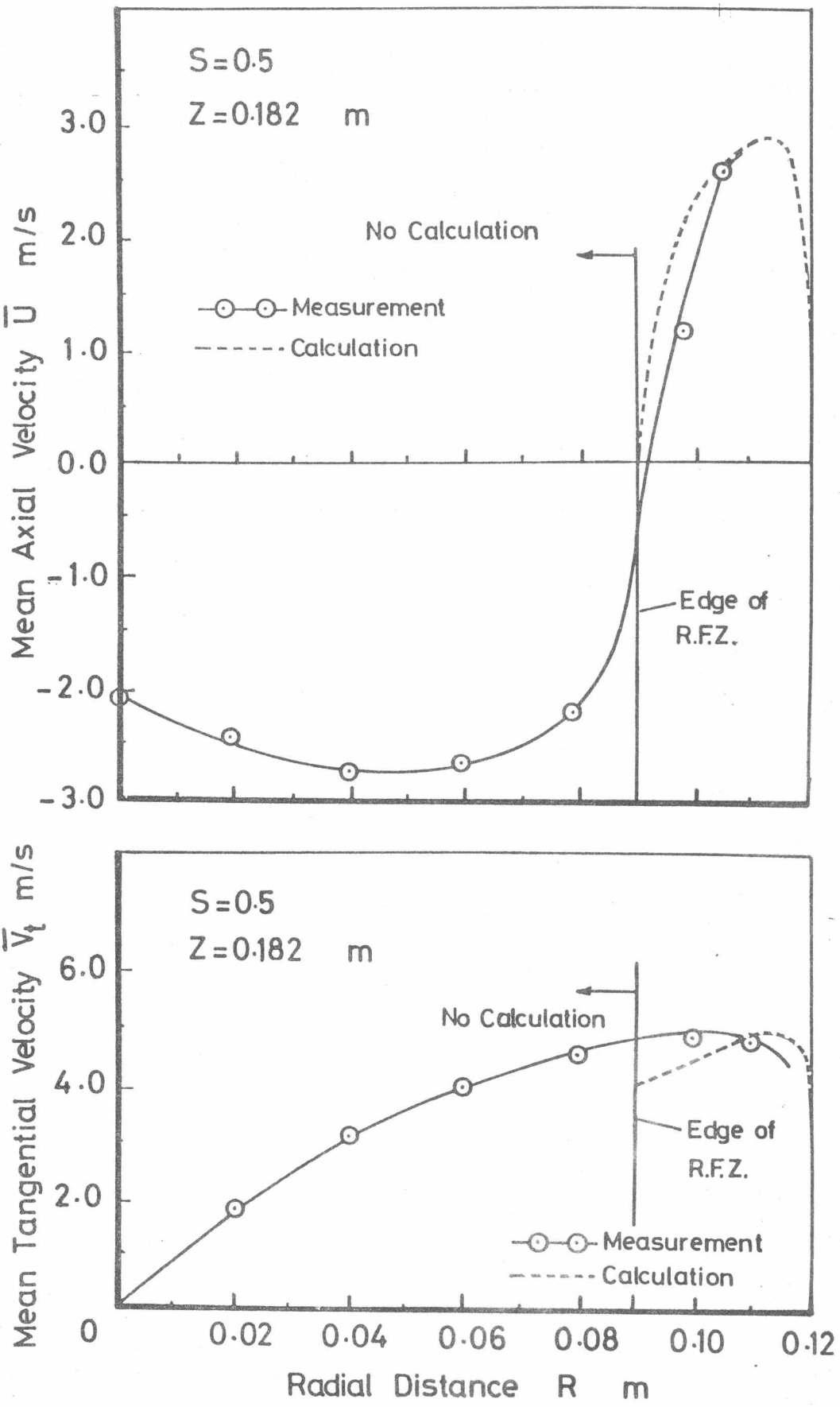

Fig.4 Comparison between measurements and calculations of mean axial and tangential velocities, for S=0.50, Z=0.182 m

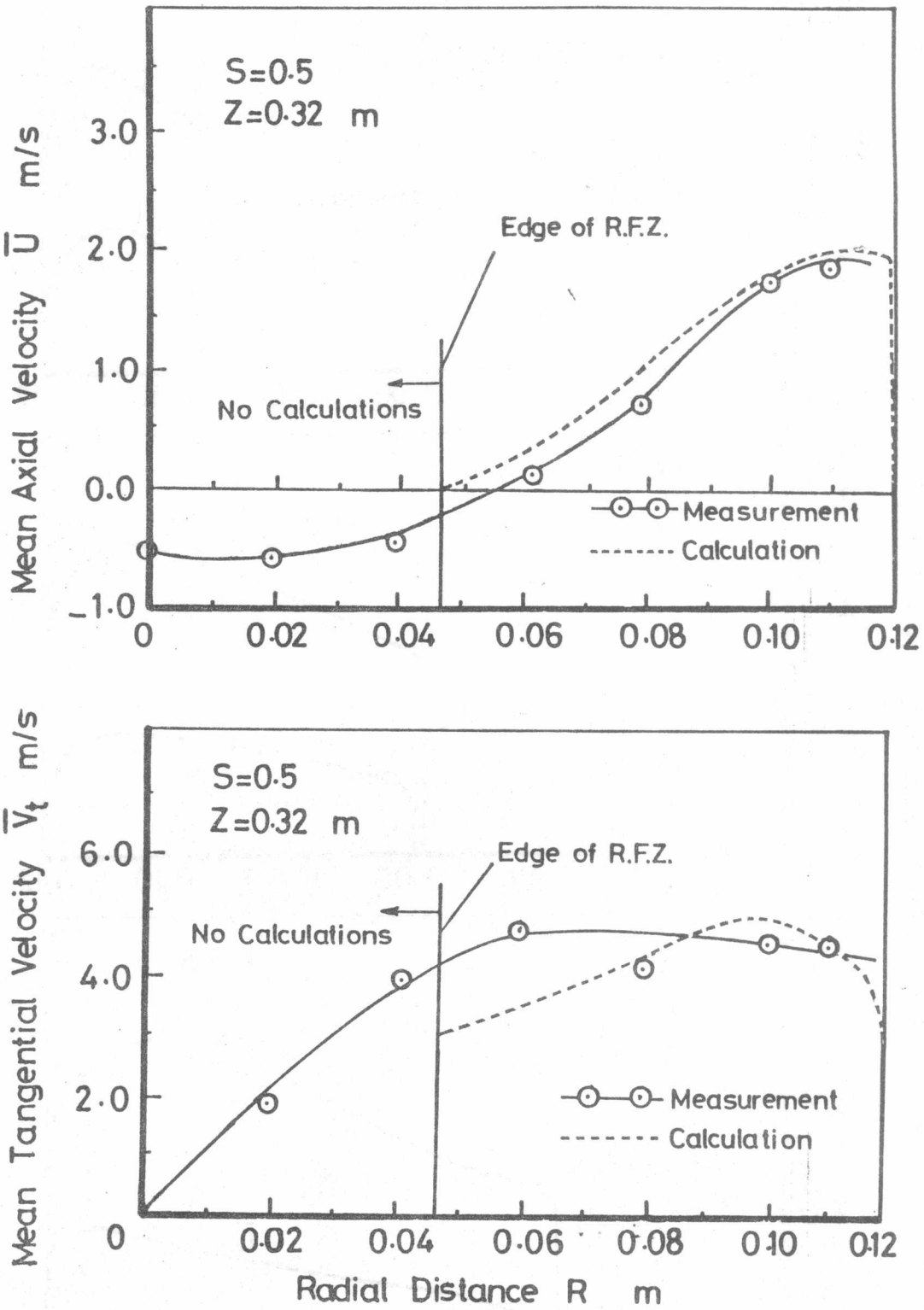

Fig.5 Comparison between measurements and calculations of mean axial and tangential velocities , for S=0.50, Z=0.32 m

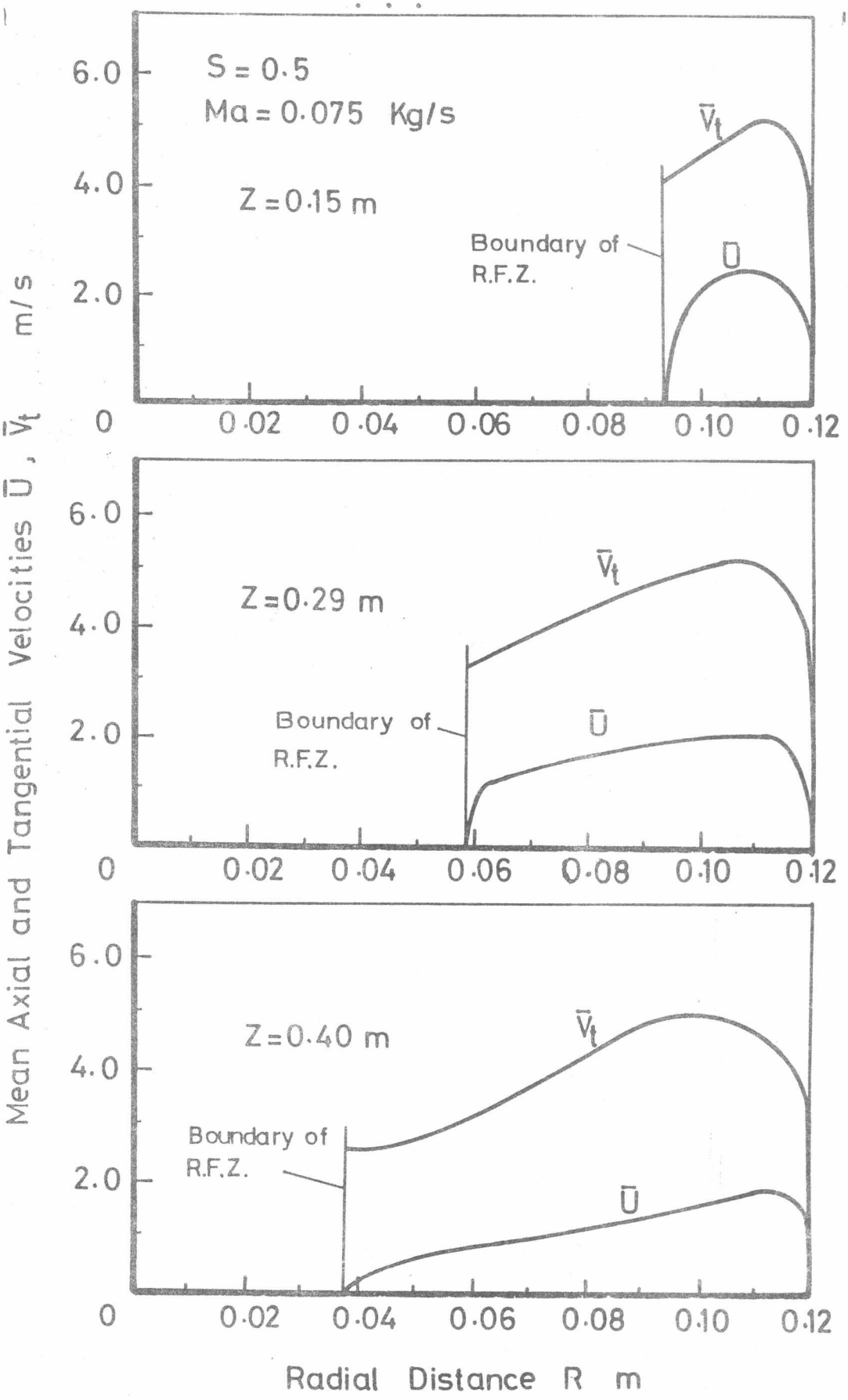

Fig.6 Distributions of the calculated mean axial and tangential velocities at different axial distances for S=0.50

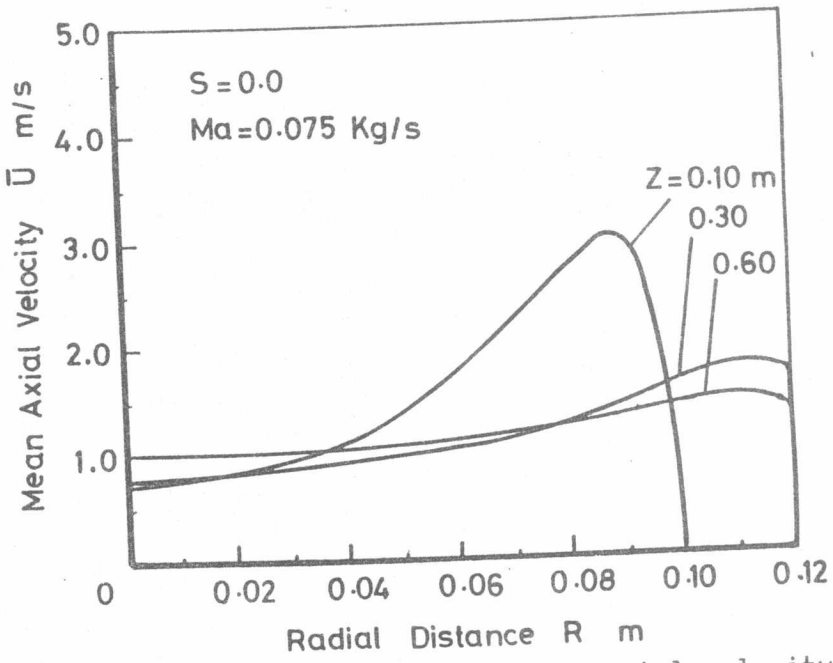

Fig.7 Distributions of the calculated mean axial velocity with radial distance at different axial distances for S=0.0

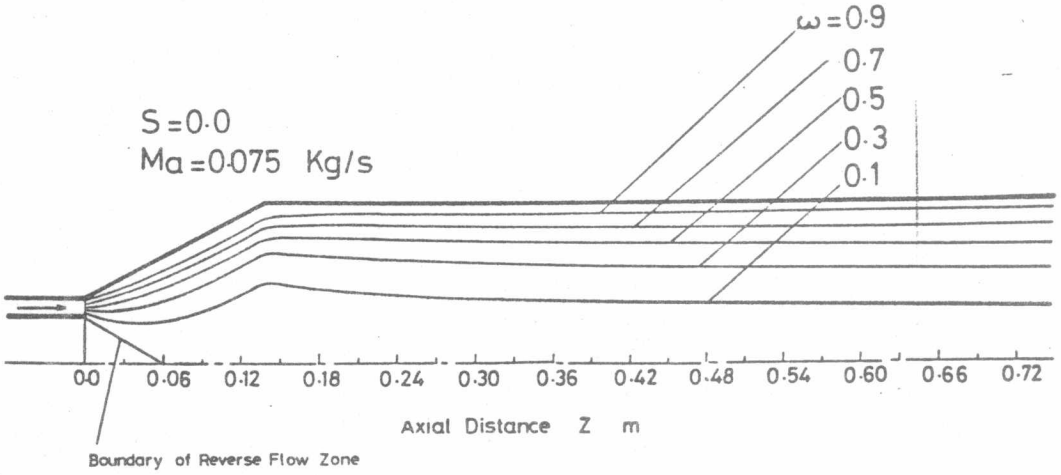

Fig.8 Calculated dimensionless stream lines for S=0.0 (without swirl)

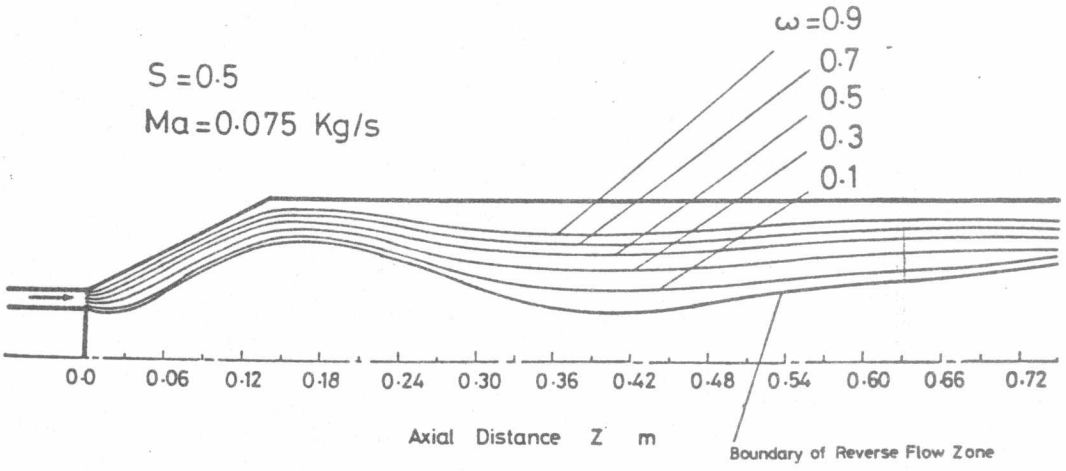

Fig.9 Calculated dimensionless stream lines for S=0.50 (with swirl)